IV International Conference on Particle-based Methods – Fundamentals and Applications
PARTICLES 2015
E. Oñate, M. Bischoff, D.R.J. Owen, P. Wriggers & T. Zohdi (Eds)

USING THE DIPOLE PARTICLES FOR SIMULATION OF 3D VORTEX FLOW OF A VISCOUS INCOMPRESSIBLE FLUID

DMITRII A. SYROVATSKII[1], GALINA YA. DYNNIKOVA[1], SERGEY V. GUVERNYUK[1,2], AND GURGEN ARUTUNYAN[2]

[1]Research Institute of Mechanics, M. V. Lomonosov Moscow State University
Michurinskii pr. 1, Moscow, 119192, Russia
[sd, dyn, guv]@imec.msu.ru, guv@imec.msu.ru

[2] T-Services,
Leninskii pr. 113/1, 117198 Moscow, Russia
gurgen.arutunyan@t-services.ru

Key words: Meshfree numerical method, three dimensional flow, dipole particles, impuls formulation, incompressible flow.

Abstract. A fully lagrangian numerical method for simulation of 3D nonstationary flow of viscous and ideal incompressible fluid is developed in this work. This method is based on the representation of a vortex field as a set of dipole particles [1]. The introduced vector-function D describes density of dipole momentum. The equation for this function is in accordance with Navier-Stokes equations [2]. The vorticity is equal to curl of dipole momentum density. Thus vortex field is always solenoidal. The dipole particles are generated at a body surface and are moving interacting. The region where function D is essentially non-zero approximately coincides with the vortex region. Each dipole particle induces the velocity field which is equal to field of a point dipole at large distance from the particle. But near a particle the induced velocity field is another taking into account the particle volume and viscosity of the liquid. The method can be applied for simulation of an ideal and viscous flows.

1 INTRODUCTION

Simulation of 3D vortex flow in 3-D space has the problem of the representation of three-dimensional vortex field by discrete elements. This field must be divergence-free as a curl of velocity field. But when the discrete vortex particles are used, this property can be destroyed. The velocity field which the vortex particle induces in accordance with Biot-Savart formula has non-zero vorticity in the whole space but not only in the localization of the particle. If the set of the vortex particles does not form a divergence-free vector field then the rotor of the induced velocity field does not coincide with this vector field. This leads to errors in the calculation if special measures are not taken. Therefore hybrid methods are often applied with combination of the Eulerian and Lagrangian approaches [3]. After the particles have been moved, their intensities are recalculated at Euler mesh for recovering the solenoidality at each step. This procedure returns to the need to build grids, and can increase the numerical viscosity.

In this work the dipole particles are used for simulating of the 3-D vortex field. This representation provides a solenoidality of the vortex field. The fully lagrangian method of Dipole Domains (DD) is developed in [1]. Dipole distributions are widely used in hydrodynamics to calculate the potential flows (double-layer potential). The idea to construct a numerical method based on the dipole particles was suggested by Yanenko, Veretentsev and Grigoriev [4]. However, numerical realization has not been performed. Chefranov [5] used the point dipoles to model the vorticity in an ideal fluid for analyzing the mechanisms of turbulence and turbulent viscosity. It has been shown that interaction of the point dipoles in an ideal fluid can lead to explosive growth of localized vorticity. The vortex dipoles were applied in papers [6,7,8] for the simulation of the inviscid vortex flow and analyzing of the turbulence.

In the method DD the smooth dipole particles are used. Viscous interaction of the particles can be taken into account.

2 GOVERNING EQUATIONS

We use a vector function **D**, which is described by the equation

$$\frac{\partial \mathbf{D}}{\partial t} = \mathbf{V} \times \left(\nabla \times \mathbf{D}\right) + \nu\nabla^2 \mathbf{V} - \nabla\left(\mathbf{VD} - \nu\nabla\mathbf{D}\right) \tag{1}$$

V is the divergence-free function with the same curl as **D**, i.e. $\nabla\mathbf{V} = 0, \quad \nabla \times \mathbf{V} = \nabla \times \mathbf{D}$.

Applying rotor to equation (1) one obtains the equation

$$\frac{\partial\left(\nabla \times \mathbf{D}\right)}{\partial t} = \nabla \times \left(\mathbf{V} \times \left(\nabla \times \mathbf{V}\right) + \nu\nabla^2 \mathbf{V}\right). \tag{2}$$

It is evident that if in the infinite space in initial moment the function V is equal to the flow velocity with undisturbed conditions at infinity then the equality will be held further because the equation (2) for vector function $\nabla \times \mathbf{D}$ is identical with equation for $\Omega = \nabla \times \mathbf{V}$ following from Navier-Stokes equation.

Equation (1) can be transformed as following

$$\frac{\partial \mathbf{D}}{\partial t} + \left(\mathbf{V}\nabla\right)\mathbf{D} = \nu\nabla^2\mathbf{D} - \left(\mathbf{D}\nabla\right)\mathbf{V} - \mathbf{D} \times \left(\nabla \times \mathbf{V}\right). \tag{3}$$

This equation is equivalent to the equation which was used in [6,7] where it was written in the next form

$$\frac{\partial \mathbf{D}}{\partial t} + \left(\mathbf{V}\nabla\right)\mathbf{D} = \nu\nabla^2\mathbf{D} - \left(\nabla\mathbf{V}\right)^T \mathbf{D}.$$

Function **V** can be expressed via **D** with help of Biot-Savarat formula. In infinite space τ it has the form

$$\mathbf{V}\left(\mathbf{R}\right) = \frac{1}{4\pi}\int \frac{\mathbf{r} - \mathbf{R}}{\left|\mathbf{r} - \mathbf{R}\right|^3} \times \left(\nabla \times \mathbf{D}\right) d\tau + \mathbf{V}_\infty, \quad \mathbf{r} \in \tau. \tag{4}$$

Expression (4) can be transformed to following

$$\mathbf{V}(\mathbf{R})=\frac{2}{3}\mathbf{D}(\mathbf{R})+\frac{1}{4\pi}\int\left(-\frac{\mathbf{D}}{|\mathbf{r}-\mathbf{R}|^3}+\frac{3(\mathbf{r}-\mathbf{R})((\mathbf{r}-\mathbf{R})\cdot\mathbf{D})}{|\mathbf{r}-\mathbf{R}|^5}\right)\mathrm{d}\tau.$$

Here the integral is taken in the principal value. The integrand is the velocity which the point dipole located in **r** induces in the point R. That is why we call function **D** as dipole density.

Equation (3) can be solved in Lagrangian coordinates. Just as in the method VVD, the flow region with nonzero dipole density is simulated by the set of the small regions (domains). The dipole moment of each domain is $\boldsymbol{\zeta}_i = \mathbf{D}\tau_i$, where τ_i is the volume of the domain. Such domain can be considered as the particle which moves and its moment changes in accordance with equation (3). In the case of ideal fluid all dipoles move at velocity **V**, and variation of the vector $\boldsymbol{\zeta}_i$ is described by the equation

$$\frac{\mathrm{d}\varsigma_i}{\mathrm{d}t}=-(\varsigma_i\nabla)\mathbf{V}-\varsigma_i\times(\nabla\times\mathbf{V})=-\nabla(\varsigma_i\mathbf{V}),$$

$$\frac{\mathrm{d}\mathbf{r}_i}{\mathrm{d}t}=\mathbf{V}.$$

In the case of viscous fluid, the diffusion velocity can be added to the fluid velocity **V** or/and redistribution of the dipole moments can be applied.

3 TESTING THE METHOD

3.1 Simulation of a vortex ring motion in an unbounded space of ideal fluid

The following distribution function **D** was used for simulation of the vortex ring at the initial time: the components D_x and D_y are zero everywhere, D_z is equal to h^{-1} in the region where $x^2 + y^2 < 1 \cap z > z_1 \cap z < z_1 + h$, i.e. in the disk of unique radius and thickness *h*. **D** is zero outside this region. This corresponds to the thin vortex layer with the annular vortex lines at the end surface of the disc. Circulation of this vortex ring is equal to 1. In the discrete representation the disk volume is divided into domains, with dipole particles located at the nodes of a cubic grid with step $\Delta l = 0.05$ (see Figure 1. Dipole moment of every domain is $D_z = \Delta l^{\,3}/n$ where $n = 5$ is number of rows, $h = n\Delta l = 0.25$. All the particles are identical. Particles near the end surface are highlighted with a darker color. Vorticity is located near this particles and move with them, because the dipole particles and vortex tubes move in ideal fluid at velocity **V**. Each particle is smoothed by function

$$\mathbf{D}_i(\mathbf{r})=\frac{\varsigma_i}{8\pi\varepsilon_i^3}\exp\left(-\frac{|\mathbf{r}-\mathbf{r}_i|}{\varepsilon_i}\right),$$

Hence the distribution of vortisity is

$$\boldsymbol{\omega}=\nabla\times\mathbf{D}=\sum_i\frac{\varsigma_i}{8\pi\varepsilon_i^4}\times\frac{\mathbf{r}-\mathbf{r}_i}{|\mathbf{r}-\mathbf{r}_i|}\exp\left(-\frac{|\mathbf{r}-\mathbf{r}_i|}{\varepsilon_i}\right).$$

Distribution of vorticity in the cross section at initial moment is shown in Figure 1d.

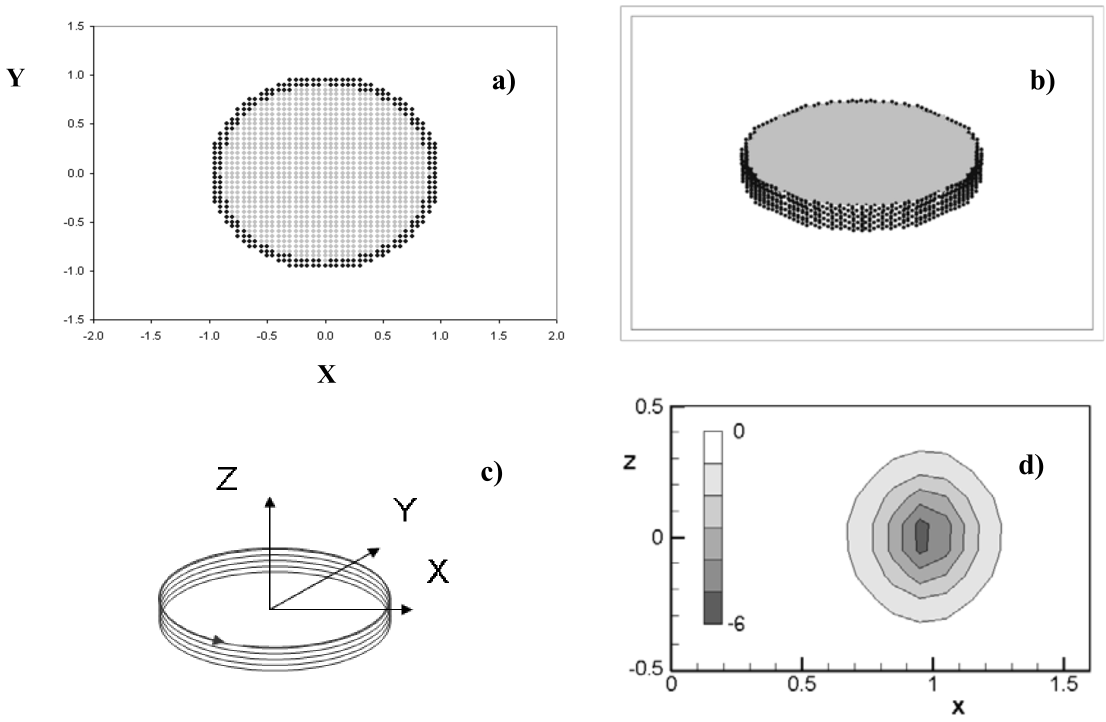

Figure 1. The initial distribution of the dipole particles (a, b); vortex lines (c); vorticity distribution in cross section (d)

In Figure 2 is presented comparison of the translation velocity of the ring with experimental and theoretical data from other researchers. There are shown the velocity calculated from Kelvin and Hicks formulas. Kelvin formula for a thin cored ring with uniform circulation is [9]

$$U = \frac{\Gamma}{4\pi R_0}\left[\ln\left(\frac{8R_0}{\varepsilon_0}\right) - \frac{1}{4} + O\left(\frac{\varepsilon_0}{R_0}\right)\right] \quad (5)$$

where R_0 is ring radius and ε_0 is core radius ($\varepsilon_0/R_0 << 1$). Here $\varepsilon_0/R_0 = 0.3$. In formula of Hicks the coefficient 1/4 in (5) is replaced by 1/2. This formula is derived for stagnant fluids inside of the core [10]. Also there are shown the numerical results of Kudela and Kossior [11], who used the Euler-Lagrange method for the ring with uniform circulation inside the core at $\varepsilon_0/R_0 = 0.3$. It should be noted that in inviscid fluid the velocity of the vortex ring with equal geometric characteristics is a linear function of the circulation. If the integration step is inversely proportional to the circulation then a linear relationship must be in accordance with the similarity laws. Deviation from linearity of the results [11] is due to the numerical viscosity probably. Our result is shown by the marker “+”.

Evolution of the distribution of dipoles near plane XZ ($-0.1 < Y < 0.1$) at successive times is presented in Figure 3. Dipole moments are shown by arrows.

The main difficulty of the dipole method is the providing the stability of the numerical scheme. Chefranov (1987) showed when two point dipoles interact, the infinite growth of the dipole moments can occur. The spread of the particles inhibits this process but it adds the numerical viscous. This question should be studied.

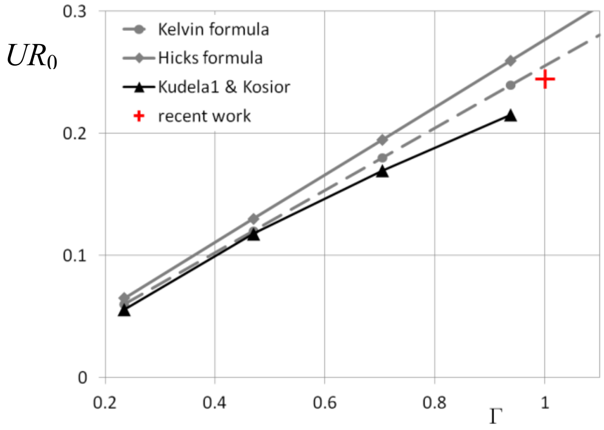

Figure 2. Comparison of theoretical and numerical velocities of vortex ring

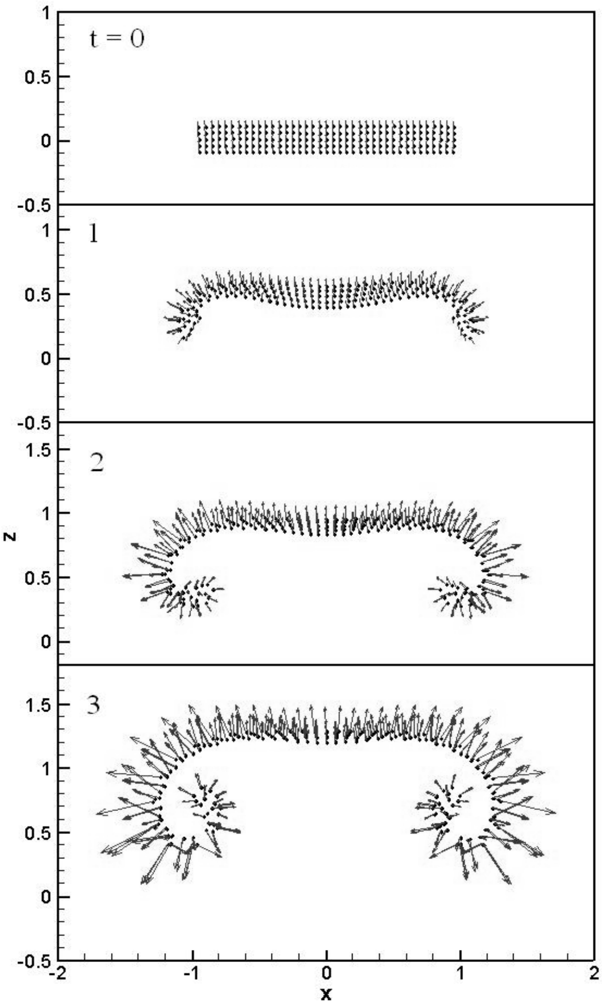

Figure 3. Evolution of the distribution of dipoles near plane XZ (– 0.1 < Y < 0.1)

3.2 Flow of ideal fluid around the thin rectangular plate at attack angle

The classical task was used for testing the method. As well as it is done by the method of Discrete Vortices, the plate is modeled by the set of discrete elements – dipole particles. The boundary condition at the plate is nonpenetration. The free dipoles are shed from the trailing edge of the plate. The attack angle varies from 1 to 5 degree. The span varies from 2 to 12.

In Figure 4 the lift coefficient dependence on the span at different attack angles is shown.

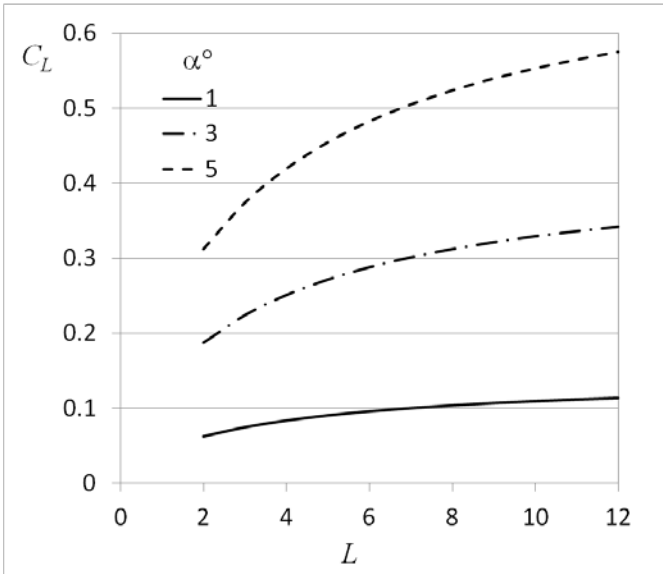

Figure 4. The lift coefficient dependence on the span at different attack angle

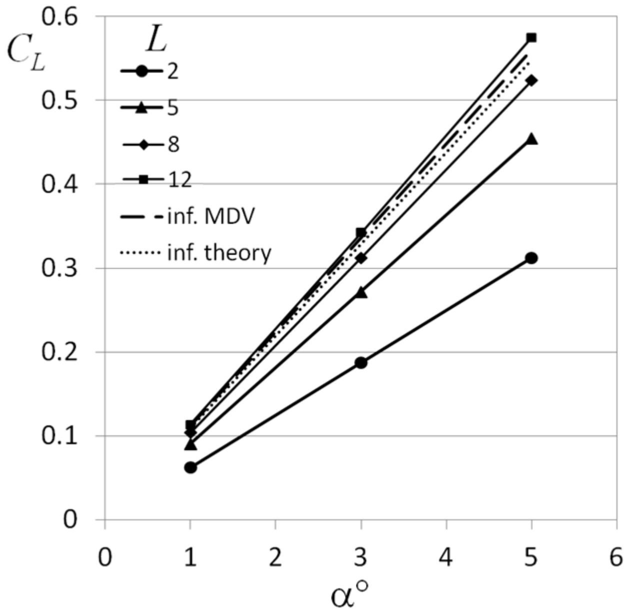

Figure 5 The lift coefficient dependence on the attack angle at different span *L*

In Figure 5 the lift coefficient dependence on the attack angle at the different span L is shown. The dashed line is obtained by method of discreet vortex (MDV) for 2D flow. The dotted line represents the theoretical curve, obtained by S.A. Chaplygin (1910) for the potential flow.

The number of discreet elements simulating the 3D plate in Figure 4 is equal to N^2L where N is the Number of particles along the horde, $N = 41$. In the case of the 2D plate simulated by MDV the number of elements along the horde is the same.

The convergence of the result with growth of the number N is shown in Figure 6 for the case $L = 6$, $\alpha = 3°$.

One can see that the values of C_L in the case $L = 12$ slightly higher than the values predicted for $L = \infty$. But as it seen at the Figure 6 the increasing of N leads to decreasing these values. Hence the accuracy can be improved by the increasing the number of discrete elements.

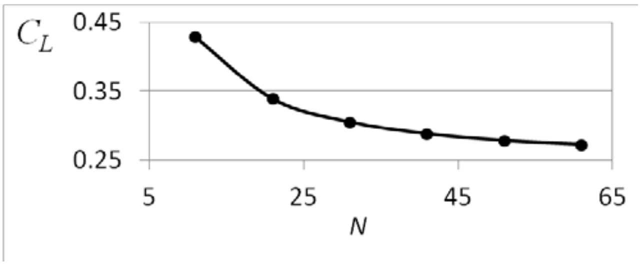

Figure 6. Convergence of the result with growth of the number of points.

4 SOME PRELIMINARY RESULTS

In this section the flow pictures without data of forces are presented as the first results obtained at the personal computer with not enough numbers of the dipole particles.

4.1 The flow of viscous fluid around the sphere

In Figure7 the formation of the separated flow around the sphere after the instant start is shown. Positions and speed of the dipoles near the plane XY passing through the center of the sphere are drawn. The Reynolds number $Re = 100$.

4.2 The ideal fluid flow generated by the propeller with one blade

The one-blade propeller starts rotation in a stationary medium. It generates the flow which carries away dipole particles generated by the blade. The scheme of the propeller is drawn in Figure 8a. The shape of the blade is depicted in Figure 8b. It consists of isosceles triangle and a semicircle. The dipole particles are shed from the trailing edge of the blade (highlighted in red). Angle of attack of the blade is 7°.

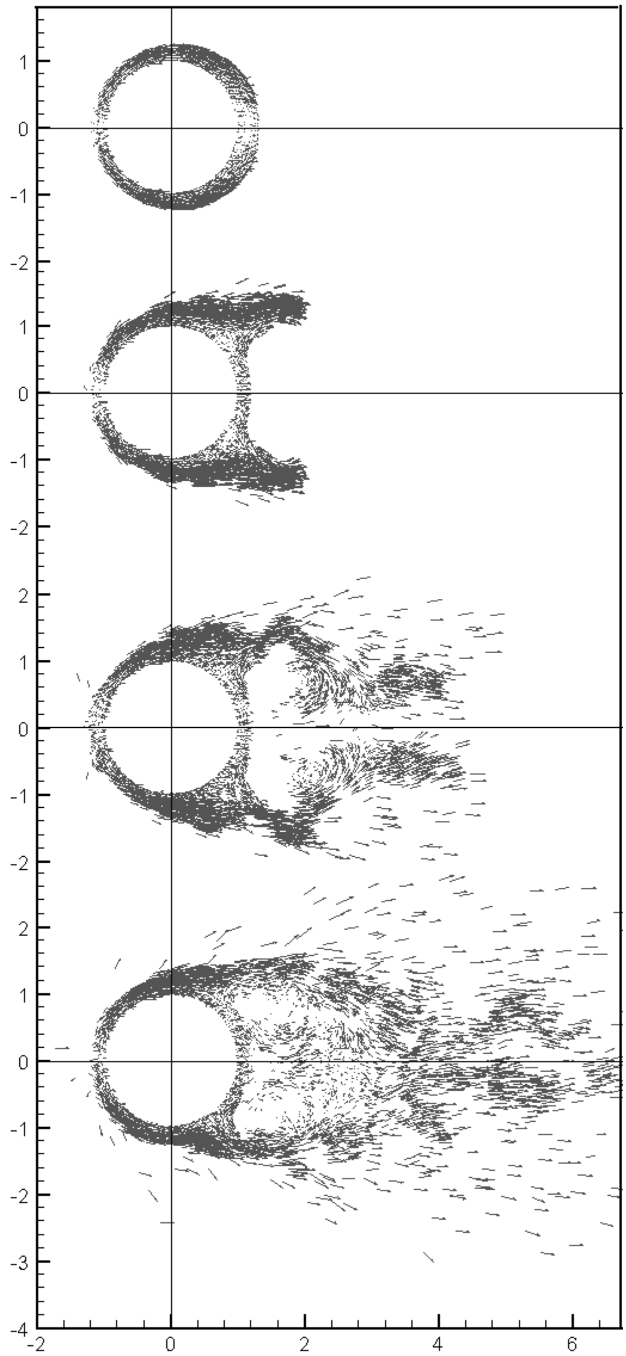

Figure 7. Formation of the separated flow around the sphere after the instant start

4.3 Oscillating plate in a flow of ideal fluid

The horizontal plate which has the form of Cassini oval performs the vertical oscillations in a horizontal flow of ideal fluid directed perpendicularly to the long axis of the oval (see Figure 9a). The Strouhal number $St = fa/U = 0.45$, where f is the frequency of the oscillations, a is the length of the short axis of the oval. The amplitude of oscillations related to a is equal to 0.085.

The dipole particles are shed from the trailing edge which is highlighted in red in Figure 9a. In Figure 9b the position of the dipole particles is depicted. The color corresponds to the height of the point.

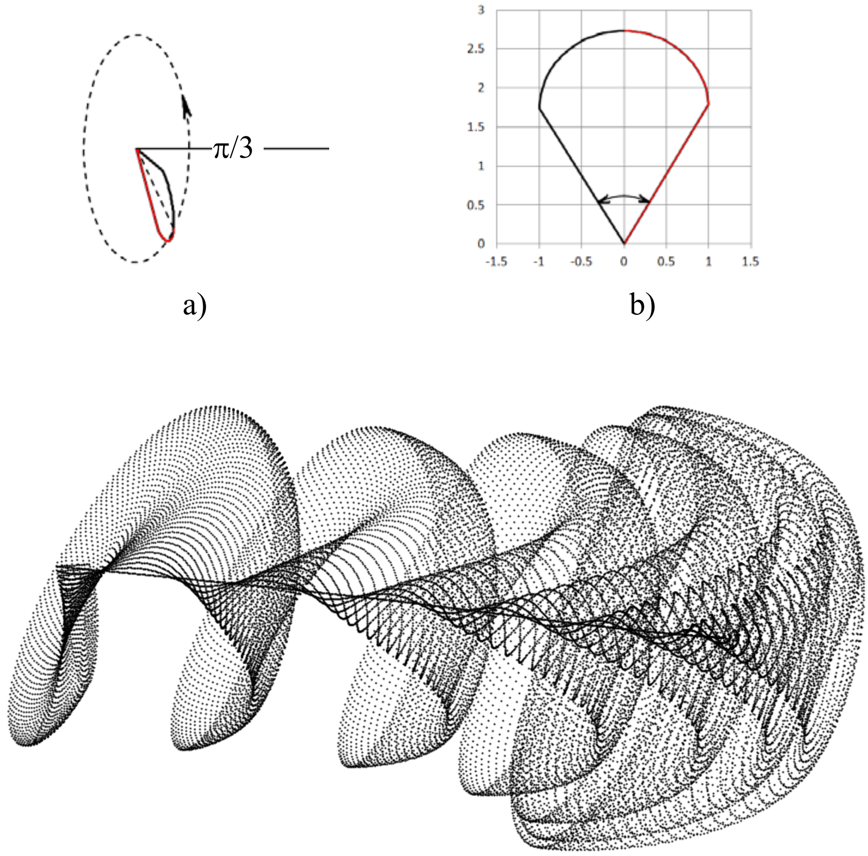

c)

Figure 8. Propeller with one blade: a) scheme of propeller, b) shape of the blade, c) position of the dipole particles

5 CONCLUSIONS

The method of Dipole Domains is perspective method for meshfree simulating 3D flow of ideal and viscous incompressible fluid. The method provides solenoidality of the vortex field and is fully lagrangian. The most important advantages of DD-method has its basis in modeling of essentially non stationary interactions of deformable bodies with the fluid.

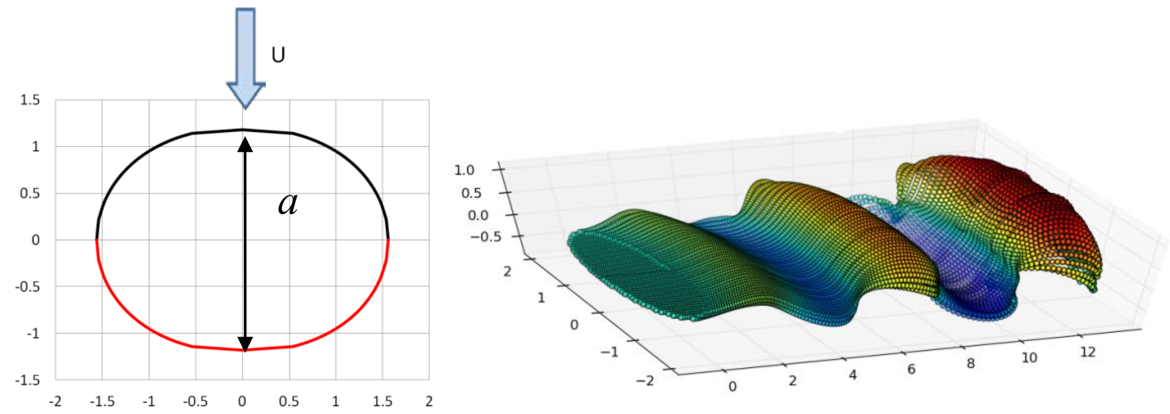

a) b)

Figure 9. Oscillating plate in a flow of ideal fluid

6 SUPPORT

The work was supported by the Ministry of Education and Science of the Russian Federation (Agreement No. 14.576.21.0079, project id RFMEFI57614X0079).

REFERENCES

[1] Dynnikova, G.Ya. *Calculation of three-dimensional flows of an incompressible fluid based on a dipole representation of vorticity*. Doklady Physics, **56**, 3, 163-166 (2011).
[2] Oseledets, V.I., *On a new way of writing the Navier-Stokes equation. The Hamiltonian formalism*, Russ.Math.Surveys, **44** 210-211 (1989).
[3] Cottet, G.H. and Koumoutsakos, P.D. *Vortex Methods: Theory and Practice.* Cambridge University Press, (2000).
[4] Yanenko, N.N., Veretentsev, A.N. and Grigoryev, Yu.N., *In: Numerical methods of Mechanics of continuous medium*. Novosibirsk, Vol. 10, p. 144, (1979), in Russian.
[5] Chefranov, S.G., *The dynamics of point vortex dipoles and spontaneous singularities in three-dimensional turbulent flows.* Journal of Exp. And Theor. Phys. (ISSN 0044-4510), Vol. 93, pp. 151-158, (1987), in Russian.
[6] Buttke, T.F. and Chorin, A.J., *Turbulence calculations in magnetization variables*, Appl. Numer. Math., 12 (1993), pp. 47–54.
[7] Cortez, R., *On the accuracy of impulse methods for fluid flow*. SIAM J. Sci. Comput. Vol. 19, No. 4, pp. 1290–1302, July (1998).
[8] Newton, P.K., *The dipole dynamical system.*Discret and continuous dynamical systems. Supplement Volume (2005) pp. 692-699.
[9] Green, S. I., *Fluid Vortices*, Springer, (1995).
[10] Saffman, P. G., *Vortex Dynamics,* Cambridge University Press, (1992).
[11] Kudela, H. and Kosior, A. *Modeling vortex rings dynamics with vortex in cell method*, Journal of Physics: Conference Series, 318, 062014, doi:10.1088/1742-6596/318/6/062014, 2011.